Kondo screening regimes of a quantum dot with a single Mn ion

E. Vernek,[1] Fanyao Qu,[2] F. M. Souza,[1] J. C. Egues,[3] and E. V. Anda[4]
[1]*Instituto de Física, Universidade Federal de Uberlândia, Uberlândia, MG 38400-902, Brazil*
[2]*Instituto de Física, Universidade de Brasília, Brasília, DF 70919-900, Brazil*
[3]*Departamento de Física e Informática, Instituto de Física de São Carlos, Universidade de São Paulo, 13560-970 São Carlos, São Paulo, Brazil*
[4]*Departamento de Física, Pontifícia Universidade Católica, Rio de Janeiro-RJ, Brazil*
(Received 2 February 2011; revised manuscript received 7 April 2011; published 23 May 2011)

We study the Kondo and transport properties of a quantum dot with a single magnetic Mn ion connected to metallic leads. By employing a numerical renormalization group technique we show that depending on the value of ferromagnetic coupling strength between the local electronic spin and the magnetic moment of the Mn, two distinct Kondo regimes exist. In the weak-coupling limit, the system can be found in a completely screened Kondo state describing a local magnetic moment *decoupled* from the rest of the system. In contrast, in the strong-coupling regime the quantum dot spin and the local magnetic moment form a single *large-spin* entity partially Kondo screened. A crossover between these two regimes can be suitably tuned by varying the tunnel coupling between the quantum dot and the leads. The model investigated here is also suitable to study magnetic molecules adsorbed on a metallic surface. The rich phenomenology of these systems is reflected in the conductance across the system.

DOI: 10.1103/PhysRevB.83.205422 PACS number(s): 72.10.−d, 73.21.La, 73.23.Hk, 75.50.Pp

I. INTRODUCTION

Spin manipulation of localized impurities is of great interest in spintronics and quantum computation.[1] In this context, diluted magnetic semiconductor quantum dots (DMSQDs) could play a prominent role as they allow the control of the spins of the magnetic ions.[2–4] In general, DMSQDs are grown in II-VI semiconductor composites with a few Mn atoms in each quantum dot (QD).[5] In these systems, the coupling between the spins of the electrons in the QD and those of the manganese arises from the *sp-d* exchange interaction.

More recently, the successful fabrication of QDs doped with a single Mn^{2+} ion[6–8] has stimulated many optical and transport measurements,[9–11] demanding a great deal of theoretical efforts.[12–15] Recent investigations of these systems have uncovered many interesting physical phenomena.[6,8–11,16–19] For instance, the exchange interaction makes single photon emitters active at six different frequencies, thus serving as the basic framework for the six-state qubit.[13] In this context, a very exotic system composed of an "impurity" with spin degrees of freedom coupled to a QD containing electrons (the impurity is outside the QD) has been proposed and studied recently.[18] Fewer theoretical works, however, have addressed the transport properties in these systems.[20]

In this paper we investigate the low-temperature properties of a QD with a single magnetic Mn ion connected to leads. The study could be applied as well to analyze magnetic molecules[21] containing sites with correlated electrons, adsorbed on a metallic surface or connected to independent leads. Although the ideas have this general scope, to be concrete, we restrict our discussion to a system composed of a Mn^{2+} ion in a small QD, coupled to two metallic (source and drain) leads, schematically represented in Fig. 1. It is well known that a QD connected to leads possesses a Kondo ground state similarly to what happens in magnetic impurities embedded in metals under temperature below the characteristic Kondo temperature (T_K).[22–24] Simultaneously, the electrons in the QD couple to the Mn^{2+} magnetic moment by a *ferromagnetic* exchange interaction J that can be optically or electrically tuned.[15,16] The antiferromagnetic case will be discussed in detail elsewhere.[25] In our case, T_K can be modified by tuning the hopping matrix element V that connects the localized and the lead states, while J in turn can be tailored by properly choosing the size of the QD.[19]

Based on a numerical renormalization group (NRG) technique,[26,29] our theoretical study shows two-distinct Kondo regimes: (i) $T_K/|J| \gg 1$, where the QD spin is completely screened by the conduction spins comprising a Kondo state and the Mn^{2+} is *decoupled* from the rest of the system and (ii) $T_K/|J| \ll 1$, in which the spins of the electrons in the QD strongly couples to the Mn^{2+} spin, forming a *large-spin* local magnetic impurity that is partially screened by the conduction electrons: the underscreened Kondo state. Although this particular regime has been studied before with other models,[27,28] we focus our attention to the crossover between the two regimes that can be analyzed in a controllable way, modifying the Kondo temperature by suitably tuning the parameters of the system. Moreover, we present a discussion of the underlying physics and show that the conductance[30] is the appropriate physical quantity to be studied since it clearly reflects the properties of the two regimes and the crossover region.

This paper is organized in the following way: In Sec. II we describe the model and briefly discuss the numerical method.

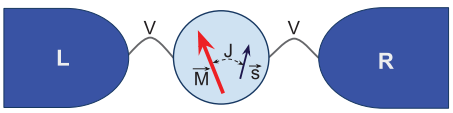

FIG. 1. (Color online) Schematic representation of a single-level quantum dot with a Mn ion. The large arrow ($\vec{M}$) represents the spin of the Mn^{2+} while the small arrow ($\vec{s}$) represents the spin of an electron in the dot. The matrix element V allows for electrons to hop in and off the quantum dot.

The numerical results are shown in Sec. III. Finally, in Sec. IV we present our concluding remarks.

II. HAMILTONIAN MODEL AND METHOD

Our system is described by the Hamiltonian $H = H_{\rm imp} + H_{\rm bands} + H_T$, where

$$H_{\rm imp} = \sum_\sigma \varepsilon_{d\sigma} c^\dagger_{d\sigma} c_{d\sigma} + U n_{d\uparrow} n_{d\downarrow} + J\mathbf{M}\cdot\mathbf{s} \qquad (1)$$

corresponds to the single-level QD and the Mn^{2+} ion, in which the operator $c^\dagger_{d\sigma}$ ($c_{d\sigma}$) creates (annihilates) an electron of spin σ with energy ε_d, U is the local Coulomb repulsion, and $\mathbf{M}$ and $\mathbf{s}$ are the spin operators of the Mn^{2+} ion and of an electron in the QD, respectively. The Hamiltonian

$$H_{\rm bands} = \sum_{\ell k\sigma} \varepsilon_{\ell k} c^\dagger_{\ell k\sigma} c_{\ell k\sigma} \qquad (2)$$

describes the conduction band, where $c^\dagger_{\ell k\sigma}$ ($c_{\ell k\sigma}$) creates (annihilates) an electron with momentum k, energy $\varepsilon_{\ell k}$, and spin projection σ in the ℓth lead ($\ell = L, R$). The conduction bands are characterized by a constant density of states given by $\rho_0(\omega) = (1/2D)\Theta(D - |\omega|)$, where D is the half bandwidth and $\Theta(x)$ is the Heaviside function. Finally,

$$H_T = \sum_{\ell k\sigma} V_\ell c^\dagger_{d\sigma} c_{\ell k\sigma} + \text{H.c.} \qquad (3)$$

describes the coupling between electrons in the QD and reservoirs.

Within the NRG framework we are able to calculate the relevant physical quantities, such as the entropy, the local magnetic moment, and the local retarded Green's function at the QD site. The latter is necessary to calculate the zero-bias conductance.

Here we mainly focus on investigating the particle-hole symmetric case ($\varepsilon_d = -U/2$) and normal leads. We take D as the energy unity. In order to illustrate the underlying physics, we start off by briefly discussing a simplified model, i.e., an isolated impurity ($V = 0$ in our model). In a single-electron QD, the spin is $s = 1/2$. Due to the vanishing angular momentum, there is no direct influence of the crystal field on the ground state of the Mn ion. Thus, the ground state of the Mn is sixfold spin degenerate. The coupling of the spin of the QD electron with the spin of the Mn^{2+} leads to a total spin momentum $\mathbf{L} = \mathbf{M} + \mathbf{s}$, with a total momentum quantum number, $l = |M - s|, \ldots, |M + s|$. For the electron-$Mn^{2+}$ complex, the possible values of l are 2 and 3. Assuming a ferromagnetic coupling $J < 0$, the ground state has $l = 3$ with degeneracy $2l + 1 = 7$, corresponding to the projections of the total angular momentum $\mathbf{L}$ along the z axis, $l_z = -3, -2, \ldots, 2, 3$.

III. NUMERICAL RESULTS

We start our numerical analysis by studying the impurity contribution to the entropy and the magnetic moment, defined, respectively, as $S(T) = S_t(T) - S_0(T)$ and $\mu^2(T) = k_B T[\chi_t(T) - \chi_0(T)]$, where χ is the magnetic susceptibility. The subscripts t and 0 refer to the quantities calculated for the entire system and in the contribution of the conduction band alone, respectively. We calculate these quantities within the usual NRG methodology.[31] Similarly, we calculate the spin-spin correlation $\langle \mathbf{M}\cdot\mathbf{s}\rangle$ an important quantity to characterize the system regime.

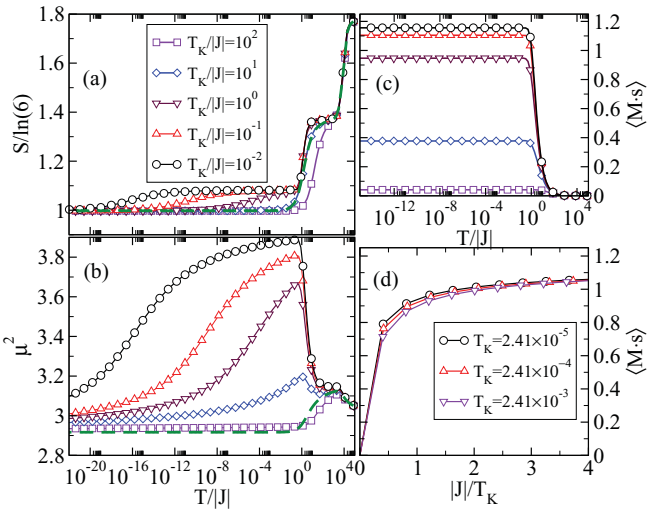

FIG. 2. (Color online) Entropy (a), magnetic moment (b), and spin-spin correlation (c) as function of temperature for various values of $T_K/|J|$, keeping $J = -2.0 \times 10^{-5}$. In the dashed (green) curve we use $J = 0$ and $T_K = 2.41 \times 10^{-4}$ and serves as a reference (for which we have scaled the temperature by 2.0×10^{-5} as in the other curves). (d) shows the spin-spin correlation as function of J/T_K for various values of T_K.

In this paper we assume $U = 0.5$ and set $k_B = \mu_B = \hbar = 1$. In Figs. 2(a) and 2(b) we show, respectively, the effects of the ferromagnetic exchange interaction and temperature on the magnetic moment and entropy for $J = -2.0 \times 10^{-5}$ and various values of V. The Kondo temperature T_K, evaluated in the absence of ferromagnetic exchange interaction, is strongly dependent on V, and can be tuned by changing V. As a reference, the $J = 0$ curve is also depicted (dashed green lines).

A. No exchange interaction

Notice in Fig. 2(a) that at high temperature $T > U$ $S \to 1.77\log(6) \approx \log(24)$, which indicates that there are $6 \times 4 = 24$ individual states, six from the Mn spin and four from the dot (spin and charge degrees of freedom), that can be thermally activated at that temperature. As the temperature decreases, the entropy presents a plateau at log(12), indicating that for $T \lesssim U/2$ the dot charge degrees of freedom are frozen. When the temperature decreases below T_K, the entropy for $J = 0$ tends to log(6) [Fig. 2(a)], indicating that the six degenerate spin states of Mn are the only contribution to the entropy because the QD electron and conduction electrons are locked into a Kondo singlet.

B. Finite ferromagnetic J case

Here the competition between the exchange interaction energy J and T_K determines the ground state of the system. The ground state is a Kondo singlet (KS) for $|J| \ll T_K$ with an uncoupled Mn ion and it becomes a local ferromagnetic

state (LFS) as $|J| \gg T_K$ due to the Mn-dot spin coupling that creates a *large spin* underscreened by the conduction electrons. Here we use the expression $T_K = \sqrt{\Gamma U}\exp[-\pi U/8\Gamma]$ to estimate the Kondo temperature of the system in the absence of the Mn atom (or $J = 0$), with $\Gamma = \pi V^2/D$ being the hybridization constant. In the intermediary case ($T_K \sim J$) the system presents a crossover region between the regimes mentioned above. In the following we analyze in detail these several regimes.

1. Small-J regime—$|J| \ll T_K$

In the regime of very weak exchange interaction, when $T \ll T_K$, the regular full screened KS state emerges. When $T < T_K$, as the temperature decreases, the KS ground state is formed by the strongly coupled dot and conduction electron spins. The characteristic of this regime is clearly illustrated in the curve for $T_K/|J| = 10^2$ □ symbol in Fig. 2(a), where almost no plateau at $S = \log(7)$ is observed. The entropy goes directly to the $S = \log(6)$ plateau. The screening of the QD-electron spin by the conduction electrons leaves the Mn-ion free. Hence the magnetic moment of the system is only due to the sixfold degenerate state of the Mn atom, which at $T = 0$ gives $\mu^2 = 2[(-5/2)^2 + (-3/2)^2 + (-1/2)^2]/6 = 35/12 \approx 2.92$, as clearly seen in Fig. 2(b) (□ curve). In order to confirm this observation, in Fig. 2(c) we show the spin-spin correlation $\langle \mathbf{M}\cdot\mathbf{s}\rangle$ as a function of the temperature using the same parameters as in Fig. 2(a). Notice that for a given $T_K/|J|$, as the temperature decreases, the correlation rapidly increases, becoming constant for $T \lesssim |J|$, indicating the formation of a large effective localized spin. For $T_K/|J| = 10^2$ the correlation remains close to zero, thus indicating that the Mn ion is almost fully decoupled from the rest of the system.

2. Large-J regime—$|J| \gg T_K$

In Figs. 2(a) and 2(b) this regime is better represented by the curve for $T_K/|J| = 10^{-2}$. In Fig. 2(a) we observe that the entropy drops to a new plateau ∼log(7) for temperatures below $|J|$ ($=2\times10^{-5}$ for this case). This new value results from the ferromagnetic coupling between the **s** and **M**. As we have discussed above, the enhancement of the magnetic moment corresponds to an unstable fixed point, characterized by a sevenfold degenerate state, corresponding to a total angular momentum $l = 3$. In this regime the QD and the Mn^{2+} ion together comprise a large local magnetic moment. This magnetic moment is, for sufficiently low temperature, partially screened by the single-channel conduction electron spins. This can be clearly seen in Fig. 2(b), where the magnetic moment is shown as a function of T. In this regime, $|J| \gg T_K$, the μ^2 is suppressed by decreasing the temperature. The local magnetic moment is only partially screened because there is only one conduction electron channel to screen the total spin. In the limit $T \to 0$ the system goes into the underscreened Kondo regime, independently of the ratio $T_K/|J|$. This is reflected in the values $\mu^2 \to 2.92$, $S \to \log(6)$, and $\langle \mathbf{M}\cdot\mathbf{s}\rangle \approx 1$, indicating a clear ferromagnetic correlation between the Mn and the dot spins. The characteristic crossover temperature T^*, below which the system can be considered to be in the underscreened regime, is shown to have a power-law dependence on $|J|/T_K$ as

$$T^* \sim (|J|/T_K)^{-\gamma}, \tag{4}$$

where γ is a positive real number. In Fig. 3 we show $\ln T^*$ as function of $\ln(|J|/T_K)$, where T^* is extracted from the magnetic moment curves of Fig. 2(b) with the condition $\mu^2(T^*) = d$, where d is a parameter that has been taken to be 3.4. Although the parameter d is to some extent arbitrary ($3 < d < 3.9$), Eq. (4) does not depend significantly upon its precise value. A similar function could have been obtained from the entropy [Fig. 2(a)]. The linear behavior of $\ln T^*$ in Fig. 3 clearly shows the power-law dependence of T^* upon J (with $\gamma = 4.75$), as written in Eq. (4). This behavior shows that T^* vanishes in the limit $J \to \infty$. Expression (4) is expected to be valid only in the underscreened regime ($|J| \gtrsim T_K$), since in the other limit the system is dominated by the regular screened Kondo regime.

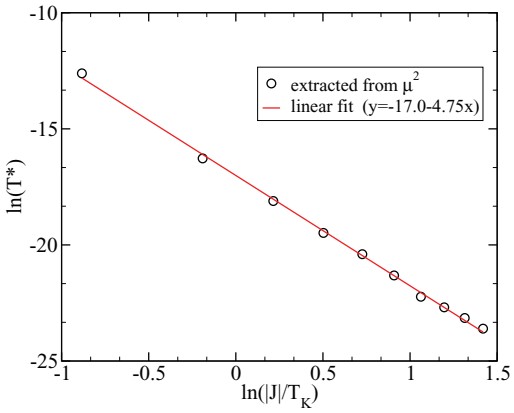

FIG. 3. (Color online) Crossover temperature T^* as function of $|J|/T_K$ showing the exponential dependence with $|J|/T_K$ as in Eq. (4). Symbols correspond to T^* extracted from μ^2 curves of Fig. 2(a) (see text), while the (red) solid line results from a linear regression for a linearized version of expression (4), which gives $\gamma = 4.75$.

3. Intermediate regime—$|J| \sim T_K$

In this case the system is in a crossover region between the two previous analyzed regimes. The amplitude of this region can be seen very clearly from Fig. 2(d), where we show $\langle \mathbf{M}\cdot\mathbf{s}\rangle$ vs. $|J|/T_K$ for three different values of T_K. Notice that the correlation rapidly increases for $|J|/T_K \lesssim 1$ and saturates slowly for larger values of $|J|/T_K$, achieving the value 5/4 for $J/|T_K| \to \infty$. The region where the correlation changes rapidly corresponds in the parameter space to the crossover region. An inspection of the figure permits to conclude that the relevant parameter that controls the moment correlations is the quantity J/T_K as we obtain the same universal function for the different values of T_K taken.

The QD density of states, $\rho_d(\omega) = -\pi^{-1}\,\mathrm{Im}[G^r_{dd}(\omega)]$, where $G^r_{dd}(\omega)$ is the Fourier transform of the double-time retarded Green's function, is calculated adopting standard NRG procedures. Within the same framework the zero-bias

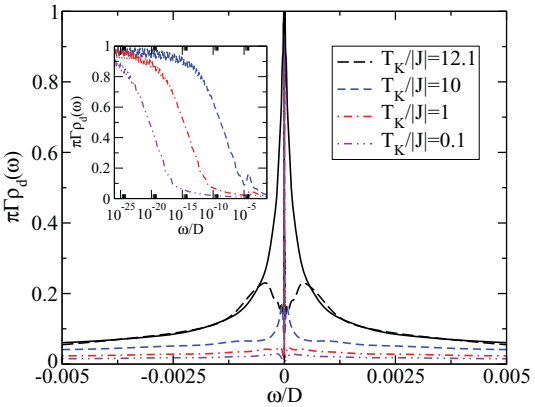

FIG. 4. (Color online) Spectral function vs ω near the Fermi level for various values of $T_K/|J|$ (fixing $J = -2 \times 10^{-5}$ and varying T_k) showing how the Kondo peak is affected due to changes in the coupling J. The line corresponds to $J = 0$ and the same T_K as in the dashed (black) line. The inset shows in a logarithmic scale the finite width of the sharp peak around the Fermi level.

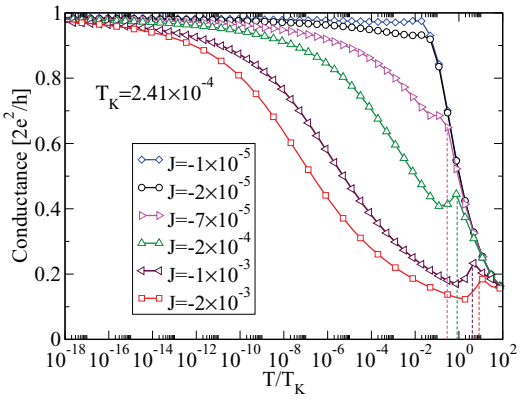

FIG. 5. (Color online) Conductance as function of temperature for various values of J and at a fixed $T_K = 2.41 \times 10^{-4}$. The vertical dashed lines indicate the position of the various $|J|$ along the x axis, showing a good coincidence with the spikes observed in the conductance.

conductance G across the QD is calculated using the Green's function formalism with the Landauer-type formula[32]

$$G = \frac{2e^2}{h}\Gamma \int_{-\infty}^{\infty} \mathrm{Im}[G^r_{dd}(\omega)]\,[-\partial f(\omega)/\partial\omega]\,d\omega, \qquad (5)$$

where $f(\omega)$ is the Fermi function.

In Fig. 4 we show $\rho_d(\omega)$ for various values of $T_K/|J|$ near the Fermi level (for $J = -2 \times 10^{-5}$ and various T_k). Notice that even for the $T_K > |J|$ (e.g., $T_K/|J| = 12.1$) line the Kondo peak split into a three-peak structure due to the coupling J (see the two satellite peaks around the Fermi level and a very sharp peak precisely at the Fermi level. The zero-frequency peak is better noticed in a logarithmic scale, as shown in the inset of the figure). The characteristic energy of this regime is given by the width of the complete three-peak structure. When compared to the solid curve for $J = 0$, we see that the change in the density of states is restricted to the Kondo peak ($\sim T_K$) region and there is a clear collapse of the two curves for $|\omega| \gtrsim T_K$. As $T_K/|J|$ decreases we see a dramatic distortion in the Kondo peak: The three-peak structure tends to disappear and essentially the density of states is dominated by the central sharp peak at the Fermi level. It is interesting to observe that, despite the strong modification of the spectral function, the height of the peak *at* the Fermi level remains $1/\pi\Gamma$, as predicted by the Friedel sum rule. As a result, no effect would be expected for the conductance at $T = 0$. However, as we discuss below, the presence of this central peak has essential consequences on the interesting behavior of the conductance as the temperature is increased.

In Fig. 5 we show the conductance as function of temperature for various values of J. We notice two distinct regimes: (i) For $J \ll T_K$ the conductance drops at $T \sim T_K$, where the effect of the temperature is to take the system out of the standard Kondo regime and (ii) for $|J| \gg T_K$ the conductance drops for much lower temperature. For intermediate values of J, such as in $|J| = 7 \times 10^{-5} < T_K$, we observe that the behavior corresponding to the two regimes is contained in the same curve. The shape of the conductance differs completely whether $T < |J|$ or $T > |J|$. The appearance of these two regimes with temperature can be understood as follows: By decreasing T, in the interval $|J| < T < T_K$, the system restores the behavior of the completely screened Kondo state at that temperature, as thermal excitations destroy the dot-magnetic atom spin-spin correlation [see Fig. 2(c)]. However, reducing T, after a crossover region, when $T < J$, the dot-magnetic atom spin degrees of freedom are coupled and the system enters an underscreened Kondo state, characterized by a conductance that is significantly dependent upon temperature.

IV. SUMMARY

We have investigated the Kondo regime of a system composed of a single Mn^{2+} ion in a QD coupled to metallic leads. Our numerical approach shows two distinct low-temperature regimes, depending on how the ferromagnetic exchange interaction J between the electrons in the QD and the magnetic moment of the Mn^{2+} compares with T_K. In the weak regime ($T_K \gg |J|$), the QD is locked in a Kondo state singlet while the magnetic moment of the Mn^{2+} decouples from the rest of the system. In the strong-coupling regime ($T_K \ll J$), the QD and the Mn^{2+} forms a spin $l = 3$ impurity that couples to the conduction band. In this case, the impurity is underscreened by the Kondo correlation with the conduction-band electrons. From the experimental point of view, Fig. 5 shows that the nature of the Kondo regime is reflected very significantly on the conductance permitting, through a transport measurement, to fully characterize the spin configuration of the system with very interesting quantum information implications. The values of temperature necessary to access the two Kondo regimes depend strongly on the parameters of the system, such as T_K and J. Although the very low values of temperature shown in Fig. 5 are out of experimental range, the conductance has a more interesting temperature dependence, which includes the crossover region, in the experimentally reachable region $T/T_K > 10^{-2}$. We

expect that our results will stimulate experimental studies of these systems and contribute to the understanding of the Kondo effect and transport in magnetic quantum dots.

ACKNOWLEDGMENT

We would like to thank the Brazilian agencies CNPq, CAPES, FAPERJ, FAPEMIG, and FAPESP for financial support.

[1] Igor Žutić, Jaroslav Fabian, and S. Das Sarma, Rev. Mod. Phys. **76**, 323 (2004), and references therein.
[2] D. P. DiVicenzo, Science **270**, 255 (1995).
[3] M. Ogura and H. Akai, Appl. Phys. Lett. **91**, 253118 (2007).
[4] A. A. Maksimov, G. Bacher, A. McDonald, V. D. Kulakovskii, A. Forchel, C. R. Becker, G. Landwehr, and L. W. Molenkamp, Phys. Rev. B **62**, 7767 (2000).
[5] P. S. Cornaglia, D. R. Grempel, and H. Ness, Phys. Rev. B **71**, 075320 (2005).
[6] L. Besombes *et al.*, Phys. Rev. Lett. **93**, 207403 (2004).
[7] L. Maingault, Appl. Phys. Lett. **89**, 193109 (2006).
[8] A. Kudelski *et al.*, Phys. Rev. Lett. **99**, 247209 (2007).
[9] D. E. Reiter, T. Kuhn, and V. M. Axt, Phys. Rev. Lett. **102**, 177403 (2009).
[10] M. Goryca *et al.*, Phys. Rev. Lett. **103**, 087401 (2009).
[11] C. Le Gall *et al.*, Phys. Rev. Lett. **102**, 127402 (2009).
[12] A. O. Govorov, Phys. Rev. B **70**, 035321 (2004).
[13] A. O. Govorov and A. V. Kalameitsev, Phys. Rev. B **71**, 035338 (2005).
[14] G. V. Astakhov *et al.*, Phys. Rev. Lett. **101**, 076602 (2008).
[15] Y. Léger, L. Besombes, L. Maingault, D. Ferrand, and H. Mariette, Phys. Rev. Lett. **95**, 047403 (2005).
[16] Fanyao Qu and Pawel Hawrylak, Phys. Rev. Lett. **95**, 217206 (2005).
[17] P. Simon, R. López, and Y. Oreg, Phys. Rev. Lett. **94**, 086602 (2005).
[18] Ribhu K. Kaul *et al.*, Phys. Rev. B **80**, 035318 (2009).
[19] Fanyao Qu and P. Vasilopoulos, Appl. Phys. Lett. **89**, 122512 (2006); Phys. Rev. B **74**, 245308 (2006).
[20] M. Misiorny, I. Weymann, and J. Barnas, Phys. Rev. Lett. **106**, 126602 (2011).
[21] P. S. Cornaglia, P. Roura Bas, A. A. Aligia and C. A. Balseiro, Europhys. Lett. **93**, 47005 (2011).
[22] D. Goldhaber-Gordon, H. Shtrikman, D. Mahalu, D. Abusch-Magder, U. Meirav, and M. A. Kastner, Nature (London) **391**, 156 (1998).
[23] H. C. Manoharan, C. P. Lutz, and D. M. Eeigler, Nature (London) **403**, 512 (2000).
[24] A. C. Hewson, *The Kondo Problem to Heavy Fermions* (Cambridge University Press, Cambridge, UK, 1993).
[25] $J > 0$ is also of interest and is left for a future investigation. See also Ref. 20.
[26] K. Wilson, Rev. Mod. Phys. **47**, 773 (1975); R. Bulla, T. A. Costi, and D. Vollhardt, Phys. Rev. B **64**, 045103 (2001).
[27] R. Žitko, J. Phys. Condens. Matter **22**, 026002 (2010).
[28] W. Koller, A. C. Hewson, and D. Meyer, Phys. Rev. B **72**, 045117 (2005).
[29] H. R. Krishna-murthy, J. W. Wilkins, and K. G. Wilson, Phys. Rev. B **21**, 1003 (1980); R. Bulla, T. A. Costi, and T. Pruschke, Rev. Mod. Phys. **80**, 395 (2008).
[30] A. C Seridonio, M. Yoshida M, and L. N. Oliveira, Europhys. Lett. **86**, 67006 (2009).
[31] We use a NRG discretization parameter $\Lambda = 2.5$ and keep 2000 states at each iteration, before accounting for the degeneracies.
[32] Y. Meir and N. S. Wingreen, Phys. Rev. Lett. **68**, 2512 (1992).